Supplementary Information: Correlated Electron Physics Near a Site-selective Pressure-induced Mott Transition in α-$LiFe_5O_8$

Samar Layek[1,2,3,*], Eran Greenberg[2,4,@], Davide Levy[2], Vitali Prakapenka[4], Siddharth S. Saxena[1,5], and Gregory Kh. Rozenberg[2,+]

[1]Cavendish Laboratory, JJ Thomson Avenue, University of Cambridge, CB3 0HE, Cambridge, UK
[2]School of Physics and Astronomy, Tel-Aviv University, 69978, Tel-Aviv, Israel
[3]Department of Physics, Applied Science Cluster, UPES, Dehradun, Uttarakhand 248007, India
[4]Center for Advanced Radiation Sources, University of Chicago, Chicago, Illinois 60637, USA
[5]British Management University, Tashkent, 35 Bobur Mirza Street, Tashkent, Uzbekistan.
[@]Present address:Applied Physics Division, SNRC, Yavne 8180000 , Israel.
[*]e-mail: samarlayek@gmail.com
[+]e-mail: emtsm@tauex.tau.ac.il

ABSTRACT

The Mott insulator-to-metal transition (IMT) driven by electron correlations has been among the main research topics in materials science over past decades. The complex interplay between electronic and lattice degrees of freedom leads to various transition scenarios. Of particular interest may be the case of a transition involving the formation of complex phases comprising regions, which differ significantly in their physical properties, within the same material. Here, we present the results which advance the understanding of the IMT phenomenon offering the documentation of a pure site-selective mechanism, not complicated by any structural and spin transformation. Combining XRD, resistivity, Mössbauer and Raman spectroscopy measurements we provide evidence for a pure pressure-induced Mott transition in α-$LiFe_5O_8$, characterized by site-selective delocalization of electrons, leading to the formation, above $\sim$65 GPa, of a site-selective Mott phase consisting of metallic and insulating sublattices. We note that the electron delocalization in the partially disordered octahedral sublattice cannot be understood purely in terms of a Mott transition, the Anderson-Mott transition picture seems more adequate.

Experimental Details

Sample preparation

A polycrystalline sample of α-$LiFe_5O_8$ was prepared by the standard solid state reaction method. Stoichiometric amounts of Li_2CO_3 (Aldrich, 99.9%) and Fe_2O_3 (Aldrich, 99.9%) were mixed, pelletized and heated at 750 °C for 12 hours in an air atmosphere within a programmable box furnace. The heating and cooling rate was kept very low in order to minimize the lithium loss and get the ordered phase respectively. A second batch of sample enriched with 25% ^{57}Fe was also prepared for high pressure MS experiments. Tel-Aviv University piston-cylinder diamond anvil cells (DACs)[1] were used for all the high-pressure measurements.

X-ray diffraction

Powder *XRD measurements* were carried out at room temperature in angle-dispersive mode at pressures up to 12 GPa at the PSICHÉ beamline of Synchrotron Soleil (Paris) and up to 83 GPa at GSECARS 13ID-D beamline of APS (Argonne), with a wavelength of λ = 0.3738 Å and 0.3344 Å, respectively. Diamond anvils with culet diameters of 400 and 200 μm were used at PSICHÉ and GSECARS for measurements up to 12 GPa and 83 GPa, respectively. Re gaskets with a starting thickness of 250 μm were pre-indented to 30 and 15 μm, and holes of 180 and 100 μm diameters were drilled at the center of the indentation, for cells of the larger and smaller culet sizes, respectively. Sample, along with spherical ruby chips and a small Pt strip, were placed at the center of the drilled cavity. Nitrogen and neon were used as pressure transmitting media for 400 and 200 μm anvil cells, respectively. Diffraction images were collected using a MAR345 image plate detector and a MAR CCD 165 detector at the PSICHÉ and GSECARS 13ID-D beamline, respectively. The diffraction images were integrated using the FIT2D[2] and DIOPTAS software[3]. Powder diffraction patterns were analyzed using the GSAS-II software[4,5] to extract the unit cell parameters.

Table S1. Birch-Murnaghan equations of state for the various phases of $LiFe_5O_8$ according to EOSfit7 software[13]. K_0, K', and V_0 are the bulk modulus, its pressure derivative, and the unit-cell volume at 1 bar and 300 K, respectively.

Phase	V_0 (Å^3)	K_0 (GPa)	K'
LP ($P4_332$)	572.5	236	4 (fixed)
HP (*Cmcm* site-selective Mott insulator)	543	313	4 (fixed)

The intensities of the diffraction peaks are affected by instrumental and sample problems (diamond x-ray absorption and low statistics in random distribution of the sample crystallites). Therefore, the Rietveld refinement of the powder diffraction patterns, particularly at high pressures, does not always result in a good enough fit. Hence diffraction patterns up to $\sim$ 30 GPa were analyzed by Rietveld refinement and above $\sim$30 GPa by using the Whole Profile Fitting (Pawley) method[6]. Whole Profile Fitting results in a reasonable fit to the data, as evidenced in Fig. 1(c) ($w_{Rp} < 0.73\%$ and 1.08, $Rp < 0.65\%$ and 1.17 for 7.1 and 61.0 GPa, respectively).

Raman spectroscopy

High-pressure *Raman spectra* of $LiFe_5O_8$ were collected at room temperature using a Horiba (iHr-550) spectrometer with a 487.8 nm excitation source at output powers up to 140 mW in the backscatter configuration with a long working distance 50x objective suitable for diamond anvil cell experiments. The spot size of the beam after focusing was about 5 μm in diameter. Collection times were in the range of 15 minutes. Collection of the Raman spectra was performed by using LabSpec software. Anvil culets of 200 μm were used, with helium serving as the pressure medium.

Mössbauer Spectroscopy

A DAC with diamond anvil culets of 200 μm, prepared in the same manner mentioned above was used for high-pressure *Mössbauer spectroscopy* measurements. N_2 was used as the pressure medium. A point-source of ^{57}Co (embedded in a Rh matrix), with an initial activity of 10 mCi was used in the transmission geometry. Low-temperature measurements down to 8 K were done using a custom made top-loading liquid nitrogen-helium cryostat. MS data were fit with a least-squares fitting to obtain the MS hyperfine parameters, including the relative abundance of the components, the chemical isomer shift, electric quadrupole splitting and magnetic hyperfine field[7]. Low temperature measurements at 76 and 90 GPa were recorded using synchrotron Mössbauer spectroscopy (SMS) measurements at ID18 beamline of ESRF using the techniques describe in[8] and He pressure medium.

Resistance measurements

High-pressure electrical *resistance measurements* up to $\sim$82 GPa were performed using a DAC with anvil culets of 200 μm diameter. A pre-pressed stainless-steel gasket was covered with an insulating layer of an Al_2O_3-NaCl mixture (3:1 atomic ratio), which also serves as the pressure medium. Samples with ruby chips were placed inside a 100 μm cavity drilled within the pressed insulating layer. Six platinum triangles (used as electrical probes for resistance measurements) placed on the other anvil were connected to copper leads, at the base of the diamond anvil, using a silver epoxy. At each pressure, for both compression and decompression cycles, resistance was measured as a function of temperature using a standard four-probe method in a custom-made cryostat. At each temperature, the voltage was measured as a function of a series of applied currents, for determining the resistance from the obtained slope.

Pressure determination

Pressure was measured both before and after each measurement from the ruby fluorescence spectra[9]. Diamond Raman spectra were also used to determine the pressure for XRD, Raman and resistance measurements[10], especially at pressures above 60 GPa. The error in the pressure determination is about 5% of the reported average pressure from the ruby fluorescence measurements. In the case of XRD studies the Ne and Pt unit-cell volumes were used for manometry[11,12].

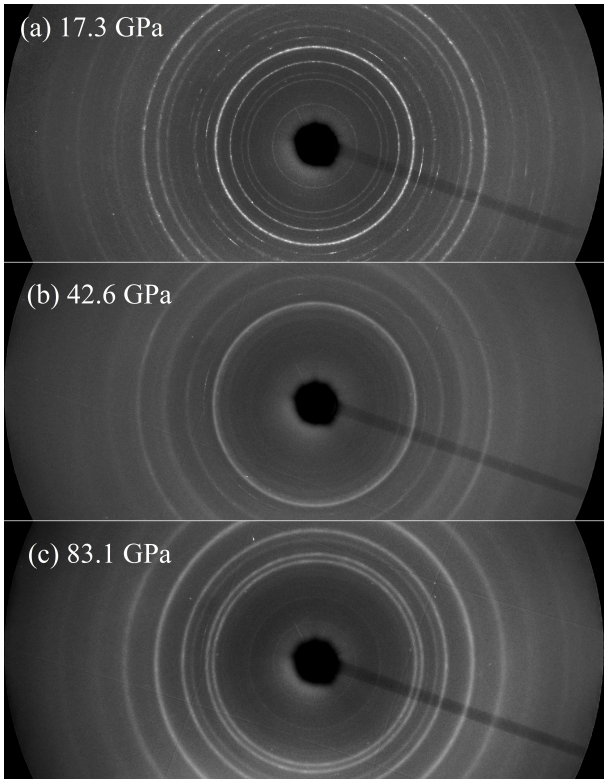

Figure S1. XRD 2D images for α-$LiFe_5O_8$ at (a) 17.3, (b) 42.6 and (c) 83.1 GPa showing structural transition from cubic $P4_332$ to orthorhombic *Cmcm* structure.

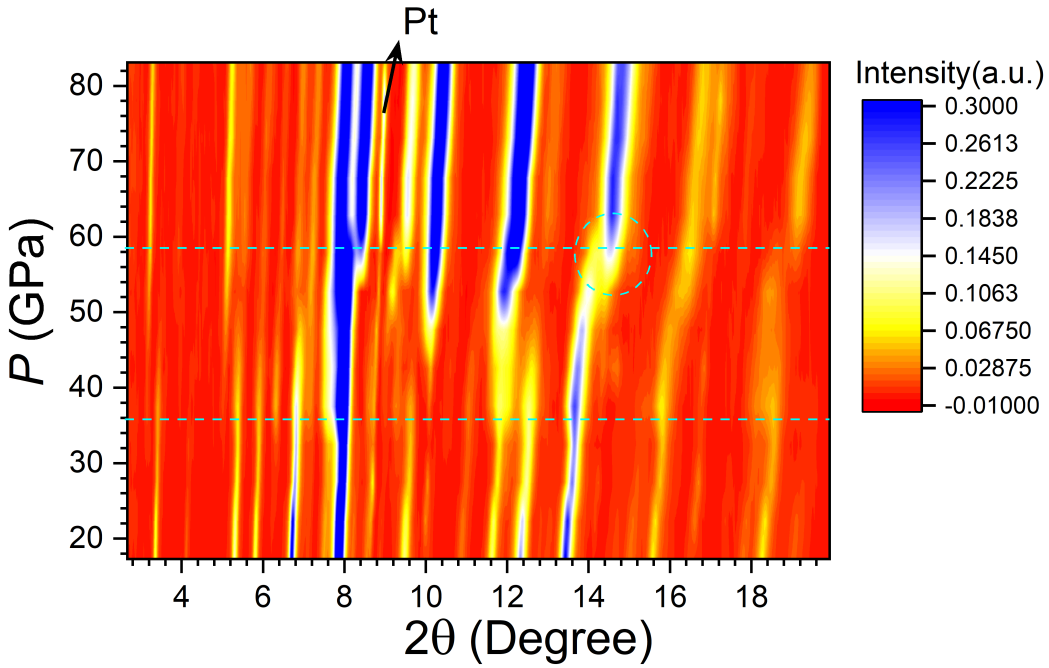

Figure S2. Contour plots of XRD patterns as a function pressure for α-$LiFe_5O_8$ clearly showing an onset of the HP phase above ~34 GPa.

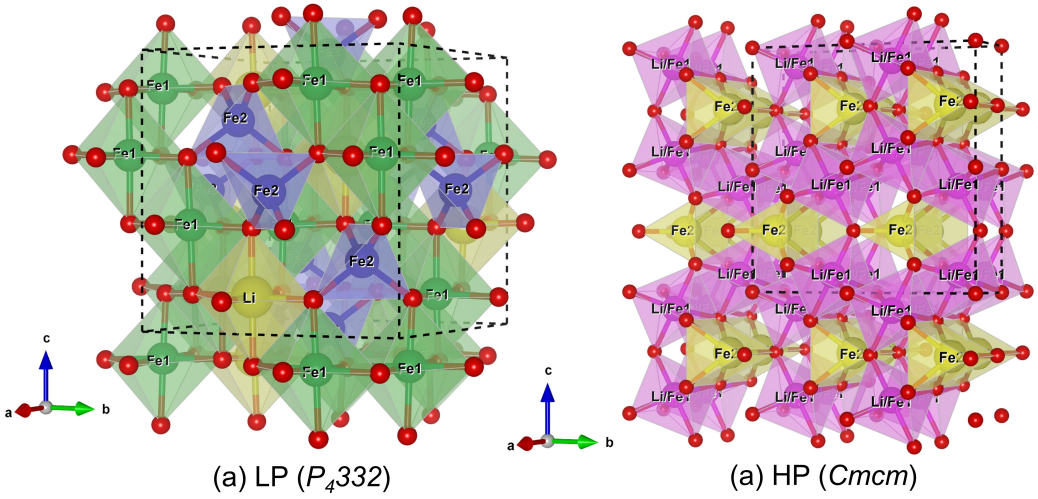

Figure S3. LP and HP crystal structure. (a) Crystal structure of the ordered spinel form of α-$LiFe_5O_8$ (space group $P4_332$ representing 8 atoms of Fe^{3+} in tetrahedral (8*c*) and 12 atoms of Fe^{3+} in octahedral (12*d*) sites, whereas 4 Li^+ ions occupy the (4*b*) octahedral positions. (b) The crystal structure of the HP *Cmcm* phase characterized by two cationic sites: octahedral (8*f*) and a bicapped trigonal prism (4*c*) Wyckoff sites, characterized by 6- and 8-fold coordination polyhedra, respectively. A part of the octahedral sites are occupied by Li^+ ions.

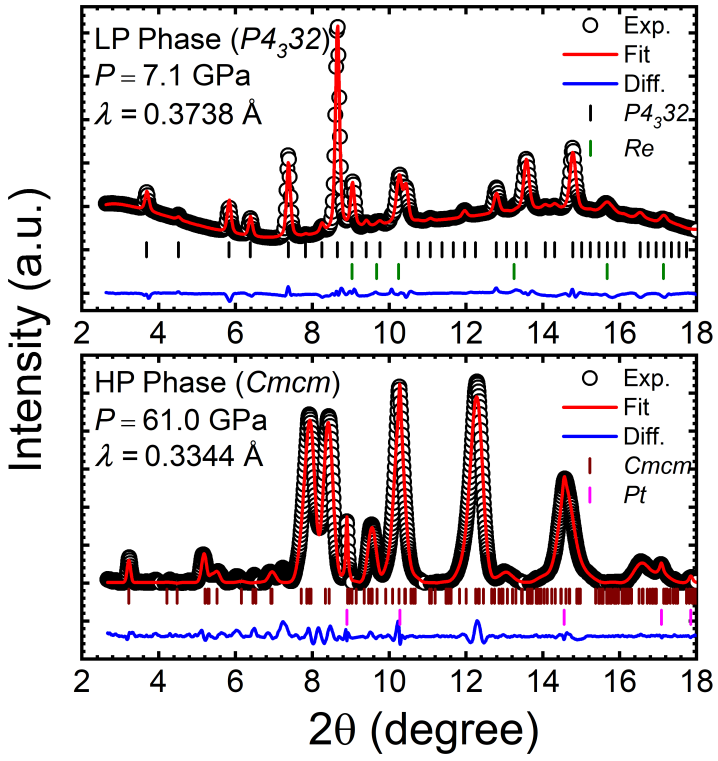

Figure S4. Refinements of representative XRD spectra, at selected pressures. Empty circles are the experimental points, solid red line is the fit, black and red bars are Bragg positions assuming the $P4_332$ and *Cmcm* space group respectively. Bragg positions of the rhenium gasket and the platinum pressure marker are indicated by green and magenta plus signs, respectively. The residuals are plotted in blue solid line at the bottom of each panel.

References

1. Machavariani, G. Y., Pasternak, M. P., Hearne, G. & Rozenberg, G. K. A multipurpose miniature piston-cylinder diamond-anvil cell for pressures beyond 100 GPa. *Rev. Sci. Instrum.* **69**, 1423–1425 (1998).
2. Hammersley, A., Svensson, S., Hanfland, M., Fitch, A. & Hausermann, D. Two-dimensional detector software: from real detector to idealised image or two-theta scan. *Int. J. High Press. Res.* **14**, 235–248 (1996).
3. Prescher, C. & Prakapenka, V. B. DIOPTAS: a program for reduction of two-dimensional x-ray diffraction data and data exploration. *High Press. Res.* **35**, 223–230 (2015).
4. Toby, B. H. EXPGUI, a graphical user interface for GSAS. *J. Appl. Cryst.* **34**, 210–213 (2001).
5. Toby, B. H. & Von Dreele, R. B. GSAS-II: the genesis of a modern open-source all purpose crystallography software package. *J. Appl. Cryst.* **46**, 544–549 (2013).
6. Pawley, G. Unit-cell refinement from powder diffraction scans. *J. Appl. Cryst.* **14**, 357–361 (1981).
7. Prescher, C., McCammon, C. & Dubrovinsky, L. MossA: a program for analyzing energy-domain Mössbauer spectra from conventional and synchrotron sources. *J. Appl. Cryst.* **45**, 329–331 (2012).
8. Potapkin, V. *et al.* The ^{57}Fe synchrotron Mössbauer source at the ESRF. *J. Synchrotron Radiat.* **19**, 559–569 (2012).
9. Dewaele, A., Torrent, M., Loubeyre, P. & Mezouar, M. Compression curves of transition metals in the Mbar range: Experiments and projector augmented-wave calculations. *Phys. Rev. B* **78**, 104102 (2008).
10. Akahama, Y. & Kawamura, H. Pressure calibration of diamond anvil raman gauge to 310 GPa. *J. Appl. Phys.* **100**, 043516 (2006).
11. Fei, Y. *et al.* Toward an internally consistent pressure scale. *Proc. Natl. Acad. Sci.* **104**, 9182–9186 (2007).
12. Dewaele, A., Loubeyre, P. & Mezouar, M. Equations of state of six metals above 94 GPa. *Phys. Rev. B* **70**, 094112 (2004).
13. Gonzalez-Platas, J., Alvaro, M., Nestola, F. & Angel, R. EosFit7-GUI: a new graphical user interface for equation of state calculations, analyses and teaching. *J. Appl. Cryst.* **49**, 1377–1382 (2016).